Antiferromagnetism in cobalt orthophosphate

1988 J. Phys. C: Solid State Phys. 21 2005

(http://iopscience.iop.org/0022-3719/21/10/018)

J. Phys. C: Solid State Phys. **21** (1988) 2005–2013. Printed in the UK

Antiferromagnetism in cobalt orthophosphate

J B Forsyth†, C Wilkinson‡, S Paster‡ and B M Wanklyn§
† Rutherford Appleton Laboratory, Chilton, Oxon OX11 0QX, UK
‡ Physics Department, King's College (KQC), The Strand, London WC2R 2LS, UK
§ Clarendon Laboratory, Oxford University, Oxford, UK

Received 2 December 1987

Abstract. Cobalt orthophosphate, $Co_3(PO_4)_2$, is known to crystallise in the monoclinic system with space group $P2_1/c$, unit-cell dimensions $a = 5.063$, $b = 8.361$ and $c = 8.788$ Å, $\beta = 121.0°$ and $Z = 2$. Susceptibility measurements show the onset of antiferromagnetism at 30.0(3) K and the magnetic structure at 4.2 K has been determined from neutron diffraction measurements on synthetic powder and single-crystal samples. The magnetic structure is commensurate with the chemical unit cell with the magnetic cell doubled along $\boldsymbol{a}$. The chemical cell contains one twofold and one fourfold site for Co^{2+} ions, whose moments lie close to $\boldsymbol{b}$ and in a more general direction within the unit cell, respectively. The refined values for the ionic moments are $Co_1 = 3.77(10)$ and $Co_2 = 3.49(7)$ μ_B, where Co_1 refers to the twofold site. The orientation of the magnetic moments is related to the spin–orbit coupling of the Co^{2+} ions and the exchange paths in the structure.

1. Introduction

Many phosphates of the first-group transition metals undergo transitions to ordered magnetic structures at low temperatures. The magnetic coupling usually results in a purely antiferromagnetic phase, although one of the hydrated phosphates of Fe(II), Ludlamite $Fe_3(PO_4)_2.4H_2O$, is remarkable in exhibiting a sizable net ferromagnetic moment due to the canting of its two coplanar antiferromagnetic sublattices. We have recently begun a series of studies whose object is to elucidate the role played by the phosphate anion group in the magnetic exchange interactions between the transition-metal ions in these materials. The anhydrous phosphates of Co(II) are particularly interesting, since the unquenched orbital moment of the cation results in strong spin–orbit coupling which influences the resulting arrangement of magnetic moments in the ordered state and may dominate the effects of magnetic exchange.

The crystal structure of $Co_3(PO_4)_2$ is relatively simple, the similarity between it and that of γ-$Zn_3(PO_4)_2$ and $Mg_3(PO_4)_2$ having been noted by Calvo (1963) and by Nord and Kierkegaard (1968) on the basis of x-ray powder photographs. Later Nord (1974) showed that the structure was closer to that of γ-$Zn_3(PO_4)_2$. Anderson *et al* (1975) refined the structure from x-ray single-crystal data collected on a diffractometer using Mo radiation. The latter authors chose to use the conventional monoclinic space group $P2_1/c$, rather than $P2_1/n$ as used by Nord, and we remain with that choice. The cell dimensions given by Anderson *et al* (1975) are

$$a = 5.063(1)\ \text{Å} \qquad b = 8.361(2)\ \text{Å} \qquad c = 8.788(2)\ \text{Å} \qquad \beta = 121.00(2)°.$$

0022-3719/88/102005 + 09 $02.50

Table 1. The fractional atomic coordinates in $Co_3(PO_4)_2$ from Anderson *et al* (1975).

Atom	10^4x	10^4y	10^4z
Co_1	0	0	0
Co_2	202(1)	3591(1)	1142(1)
P	3404(2)	6938(1)	3024(1)
O_1	2727(6)	6422(3)	4455(4)
O_2	6881(6)	6958(3)	3750(3)
O_3	1902(6)	5786(3)	1432(4)
O_4	1903(6)	8618(3)	2435(4)

Table 1 gives the fractional atomic coordinates they obtained at room temperature; Co_1 is in 2(a) at a centre of symmetry, whereas Co_2 is in a general fourfold site at $\pm(x, y, z; x, \frac{1}{2} - y, \frac{1}{2} + z)$. Figure 1 shows the linking between the Co anions and the PO_4 tetrahedra.

The measurements reported in this paper were made on a powdered sample of $Co_3(PO_4)_2$ kindly provided by Anders Nord and, later, on a single-crystal grown at the Clarendon Laboratory, Oxford, using the flux method (Wanklyn *et al* 1986).

2. Neutron powder diffractometry

The first diffraction patterns obtained on the CURRAN diffractometer at the DIDO reactor, AERE Harwell, and the D2 diffractometer at the Institut Laue–Langevin,

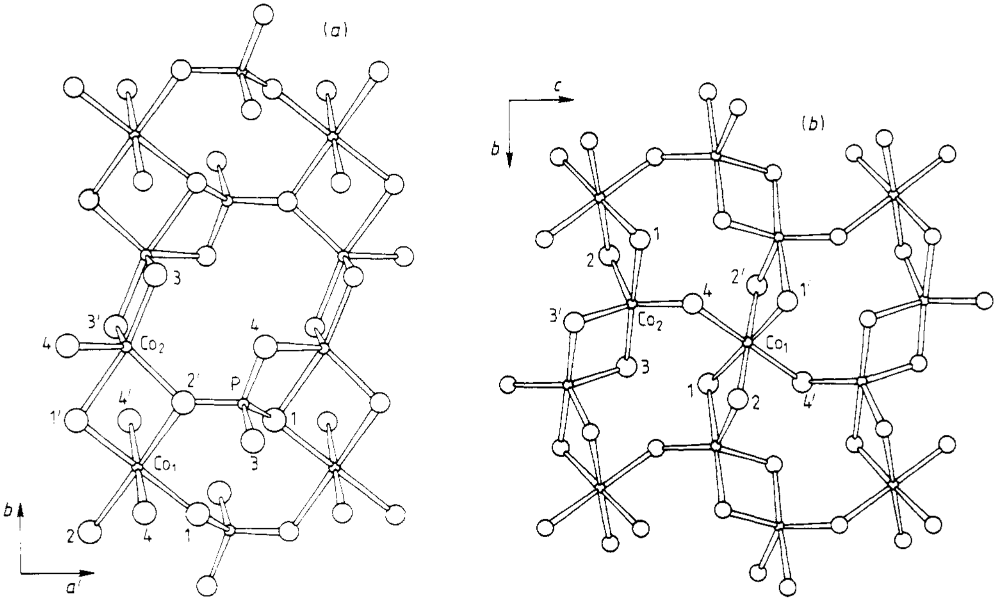

Figure 1. (*a*) The linking between Co anions and PO_4 tetrahedra in $Co_3(PO_4)_2$ projected onto the *a*–*b* plane centred about ½, ½, 0 but rotated 10° about the *b* axis for clarity, following Anderson *et al* (1975); (*b*) the linking of cobalt coordination polyhedra projected onto the *b*–*c* plane centred about the Co_1 atom at 0, ½, ½.

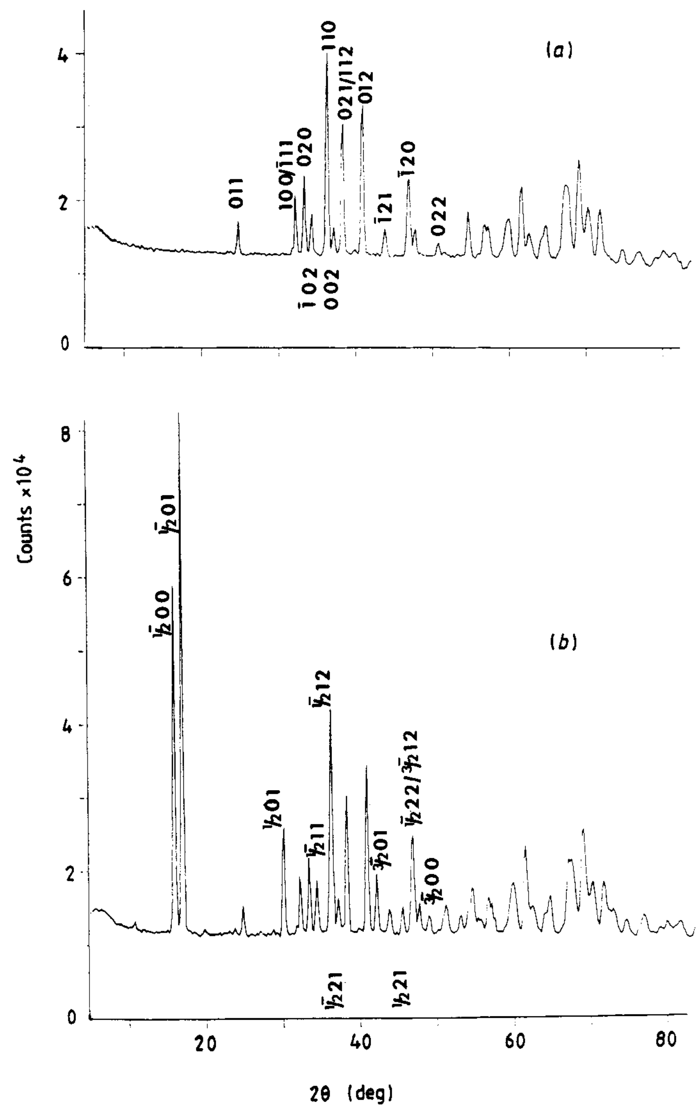

Figure 2. Powder diffraction patterns obtained at (*a*) 77 and (*b*) 4.2 K on the D1B diffractometer at the ILL.

Grenoble, showed that cobalt orthophosphate becomes magnetically ordered between the temperature of liquid nitrogen and liquid helium. A very strong, but asymmetric, line corresponding to a reciprocal-lattice vector of $\simeq 0.120$ Å^{-1} appears in the lower-temperature pattern and, on warming, disappears at 30.0(3) K. No thermal hysteresis associated with the onset and disappearance of magnetic order was observed. Further powder patterns were taken using the higher resolution of the D1B diffractometer at the ILL, with a 400-cell multidetector and an incident wavelength of 2.40 Å. Figure 2 shows the patterns obtained at 4.2 and 77 K; in the former, the two lines at $d^* \simeq 0.12$ Å^{-1} are clearly resolved and can be indexed as $(\frac{1}{2}00)$ and $(-\frac{1}{2}01)$ on the chemical unit cell. The remaining lines which feature only in the 4.2 K pattern can all be indexed in terms

Table 2. Magnetic structure amplitudes derived from D1B powder neutron diffraction measurements at a wavelength of 2.4 Å and those corresponding to the magnetic structure determined from single-crystal data.

h	k	l	F_{obs} (10^{-12} cm)	F_{calc} (10^{-12} cm)
$\frac{1}{2}$	0	0	3.13(1)	2.81
$-\frac{1}{2}$	0	1	3.91(2)	3.89
$-\frac{1}{2}$	1	0	0.28(8)	0.19
$-\frac{1}{2}$	1	1	0.39(4)	0.28
$\frac{1}{2}$	0	1	3.37(3)	3.43
$-\frac{3}{2}$	0	1	3.28(4)	3.46
$\frac{3}{2}$	0	0	2.30(7)	2.20

of a cell doubled along ***a*** and the intensities of the most significant ones are listed in table 2. Attempts to determine the magnetic structure on the basis of these observations were unsuccessful, but it seemed clear that the structure could not be collinear. The structure was finally elucidated from the single-crystal measurements reported in the next section.

3. Single-crystal measurements

Although the single-crystal sample available to us was rather large ($\approx 5 \times 5 \times 4$ mm^3), it did not exhibit clean faces and neutron Laue photographs taken on the S42 beam at

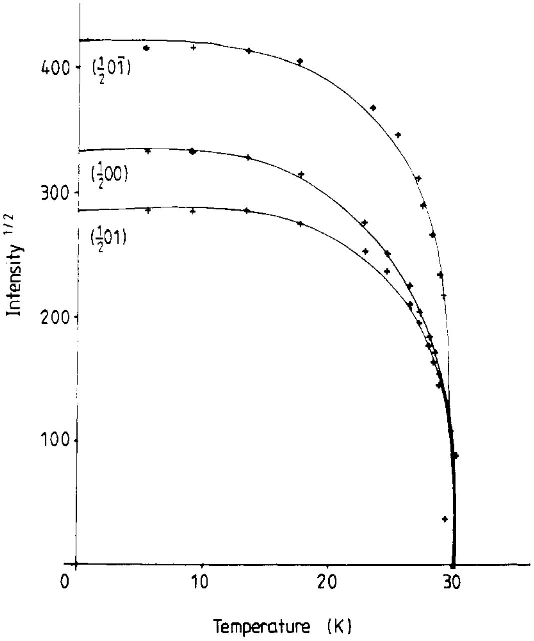

Figure 3. The temperature dependence of the magnetic ($\frac{1}{2}0-1$), ($\frac{1}{2}00$) and ($\frac{1}{2}01$) reflections in $Co_3(PO_4)_2$. The Néel temperature is 30.0(3) K.

Table 3. Observed and calculated moduli of magnetic structure amplitudes in $Co_3(PO_4)_2$. The standard deviations, $\sigma(F_{obs})$, have been determined from the agreement between equivalent reflections; the values have been given in units of 10^{-12} cm.

h	k	l	F_{obs}	$\sigma(F_{obs})$	F_{calc}
0.50	0.00	0.00	2.83	0.02	2.81
1.50	0.00	0.00	2.25	0.02	2.20
2.50	0.00	0.00	1.41	0.03	1.42
−2.50	1.00	0.00	0.25	0.11	0.34
−1.50	1.00	0.00	0.26	0.11	0.33
−2.50	2.00	0.00	0.30	0.13	0.36
−1.50	2.00	0.00	0.51	0.09	0.32
−2.50	0.00	1.00	2.58	0.02	2.49
−1.50	0.00	1.00	3.50	0.01	3.46
−0.50	0.00	1.00	3.76	0.01	3.89
0.50	0.00	1.00	3.49	0.01	3.43
1.50	0.00	1.00	2.49	0.02	2.41
−2.50	1.00	1.00	0.57	0.07	0.63
−1.50	1.00	1.00	0.94	0.03	0.83
0.50	1.00	1.00	1.17	0.03	1.16
1.50	1.00	1.00	1.17	0.06	1.06
−2.50	2.00	1.00	0.81	0.04	0.70
0.50	2.00	1.00	1.61	0.01	1.64
−0.50	0.00	2.00	0.55	0.03	0.56
0.50	0.00	2.00	0.61	0.04	0.56
−2.50	1.00	2.00	1.22	0.04	1.13
−1.50	1.00	2.00	1.67	0.02	1.66
−0.50	1.00	2.00	2.08	0.01	2.15
0.50	1.00	2.00	2.18	0.02	2.10
−2.50	2.00	2.00	1.09	0.05	1.05
−1.50	2.00	2.00	1.25	0.03	1.22
−0.50	2.00	2.00	1.11	0.02	1.22
0.50	2.00	2.00	1.53	0.02	1.47
−2.50	0.00	3.00	0.87	0.08	0.75
−1.50	0.00	3.00	0.63	0.05	0.71
−2.50	1.00	3.00	1.20	0.06	1.22
−1.50	1.00	3.00	1.39	0.02	1.55
−0.50	1.00	3.00	1.74	0.03	1.63
−2.50	2.00	3.00	0.65	0.07	0.71
−1.50	2.00	3.00	0.60	0.11	0.32
−0.50	2.00	3.00	1.04	0.03	1.13
0.50	2.00	3.00	1.84	0.03	1.45
−2.50	1.00	4.00	1.97	0.03	1.85
−1.50	1.00	4.00	2.29	0.03	2.21
−0.50	2.00	4.00	0.33	0.19	0.51
−0.50	2.00	0.00	0.18	0.07	0.15
−0.50	3.00	0.00	0.99	0.03	0.94
−0.50	2.00	1.00	0.53	0.03	0.62
−0.50	3.00	1.00	1.80	0.05	1.86
−1.50	0.00	2.00	0.22	0.12	0.26

the ILL showed that it only contained a relatively small-volume single crystal. Previous attempts to dissolve the flux of PbF_2 and PbO further had caused too much loss of single-crystal material, so we decided to use the sample as it was. No evidence was found in the diffraction peaks for the presence of a second component.

Diffractometer measurements of the integrated intensities of nuclear peaks were first made on the D9 instrument at the ILL. The instrument was fitted with a Displex cooler and the temperature was controlled at 60.0(3) K throughout two sets of measurements at 0.841 and 0.543 Å. Refinement of these data in terms of the Anderson *et al* (1975) structure and two scale factors showed extinction to be negligible and gave an agreement factor of $R = 0.026$.

The magnetic data set was measured on the D15 diffractometer, also at the ILL. This instrument was equipped with a lifting detector and the sample was mounted with a principal zone axis approximately vertical in a standard ILL 'Orange' variable-temperature liquid helium cryostat. The wavelength of the incident beam was 1.175 Å. Most data (136 reflections) were collected with the sample rotating about [010] and some 49 further reflections were measured about [101]. In both cases, nuclear reflections were included to provide an absolute scale for the magnetic intensities. The final data set of 47 independent magnetic reflections obtained from the two zones is listed in table 3, together with the standard deviations which resulted, in most instances, from the averaging of at least two equivalent reflections.

The Néel temperature of 30.0 K was also confirmed by measuring the single-crystal intensities from the $\frac{1}{2}01$, $\frac{1}{2}00$ and $\frac{1}{2}0{-1}$ reflections as a function of temperature (see figure 3).

4. Magnetic structure determination and refinement

A trial magnetic structure was determined using the magnetic Patterson function approach described by Wilkinson (1968), who showed that the height of the peak corresponding to a vector between two magnetic atoms carrying spins S_1 and S_2 is proportional to $\boldsymbol{S}_1 \cdot \boldsymbol{S}_2$ and that it is elongated parallel to the bisector of $\boldsymbol{S}_1$ and $\boldsymbol{S}_2$. Patterson sections were prepared perpendicular to [010] at the heights corresponding to the differences in y coordinate of pairs of cobalt ions. The scale of peak heights was determined from the origin peak, assuming that the ions would all have the same equal moment. The remaining vectors then provided sets of linear equations which could be solved, with some consistency, for the coupling between the ionic moments. The angle between the magnetic moments on the two Co_1 atoms, which are related by the c-glide, is essentially 180°; pairs of Co_2 atoms related by the centre of symmetry have parallel moments and the angle between pairs related by the c-glide is approximately 90°. The coupling between Co_1 and Co_2 is ferromagnetic, with an angle of about 30°. The elongation of the origin peak in the Patterson section at $y = 0.0$ indicates that the weighted direction of the components of moment in the a–c plane makes an angle of about 25° to c in β acute. It was initially assumed that the spin directions were confined to the (010) plane, since the pronounced elongation of the origin peak precludes a collinear structure with spins along [010]. However, the initial agreement between this model and the observed moduli of structure factors was only 45%, and it became clear that a fit would not be obtained without a large component of the cobalt moments being placed along [010]. This change resulted in a rapid improvement in the R-factor to some 10%. On examination, the x and z components of the Co_1 moment were found to be very small and were then constrained to be zero, and the previously independent x, y and z components of the pair of Co_2 ions were found to be similar and constrained to be equal without any worsening in the agreement factor. Finally, small x and z components of moment were reintroduced on the Co_1 ions, coupled in the same way (a c-glide with

Table 4. The components, M (in μ_B), of the Co ionic moments in $Co_3(PO_4)_2$, together with their standard deviations. The subscript to M labels the direction of the component and the fractional coordinates of the ions are also given.

Atom	10^4x	10^4y	10^4z	M_{a^*}	M_b	M_c
Co_1(A)	0	0	0	0.61(7)	−3.63(10)	−0.80(7)
Co_1(B)	0	5000	5000	0.61	3.63	−0.80
Co_2(A)	202	3591	1142	1.03(7)	−2.42(7)	−2.29(7)
Co_2(B)	9798	6409	8858	1.03	−2.42	−2.29
Co_2(C)	202	1409	6142	1.03	2.42	−2.29
Co_2(D)	9798	8591	3858	1.03	2.42	−2.29

time inversion) as the Co_2 ions. Refinement then proceeded to a final R-factor of 6.3%. The refined values of the components are listed in table 4, together with their standard deviations. The structure factors calculated from our model are in good agreement with the observed magnetic reflections in the D1B powder data, giving an R-factor of 5.3%. It should be emphasised that the Co form factor used in the refinements corresponds to a spin-only moment associated with the 3d free-ion Co^{2+} wavefunctions given by Clementi and Roetti (1974), which were fitted to a five-term analytic expression given by Lisher and Forsyth (1971).

The centre of symmetry at the Co_1 site is preserved in the magnetic structure and, since the c-glide includes time inversion, the magnetic space group is $P_{2a}2_1/c$.

5. Discussion

A more sophisticated model for the magnetisation density in $Co_3(PO_4)_2$ must attempt to include the effects of the orbital moment, which is undoubtedly present on the d^7 cobaltous ion, and the presence of covalency. The former can be modelled in the dipole approximation by replacing the zeroth-order radial integral $\langle j_0\rangle$ by $\langle j_0\rangle + [(g-2)/2]\langle j_2\rangle$, where g is the gyromagnetic ratio for the ion. The effect is to expand the form factor over that corresponding to pure spin. Changing the form factor to that for Co^+ or Co^{3+} on either or both of the Co ions and refining a value for g produced no significant improvement in the R-factor, although Co^{2+} gave the most realistic value for g (2.5). It should be noted, however, that this result could include the effect of a radial expansion of the ionic form factor in the solid state such as has been observed by Fender *et al* (1986) in ammonium manganese Tutton salt. A more exact calculation of the effect of spin–orbit coupling would be to derive the components of the ionic magnetisation directly from the ground-state wavefunction using the method described by Brown *et al* (1973) and Brown and Forsyth (1977). Unfortunately, there has as yet been no theoretical prediction made as to the appropriate wavefunction to use in this material, nor can such a calculation readily include the effects of covalency which, to first order in simple antiferromagnets, produces spin transfer to the ligand atoms resulting in spin cancellation if the ligand atom is bonded to an equal number of ions with oppositely directed moments. We consider that these difficulties, compounded with rather limited data, preclude a more detailed modelling in this case and we limit further discussion to the exchange and single-ion anisotropy in the material.

The coordination of Co_1 by oxygen is distorted octahedral and that of Co_2 is an

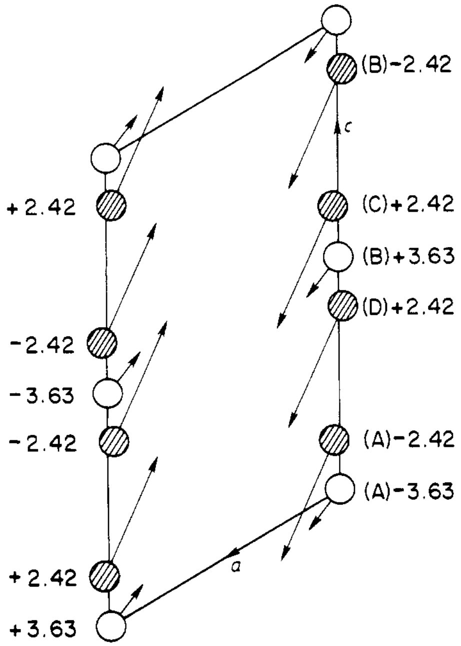

Figure 4. The orientation of the cobalt magnetic moments within one chemical unit cell of $Co_3(PO_4)_2$ projected onto the *a–c* plane. The Co_1 ions are shown as open circles and the letters in parentheses refer to the labelling in table 4. The arrows indicate the projections of the moments onto the plane: 1.00 and 2.50 μ_B for Co_1 and Co_2 respectively. The components parallel to the projection direction (3.63 and 2.29 μ_B) are also given, together with their signs.

irregular fivefold polyhedron. Two short Co–Co distances occur in the structure through the linking of these coordination polyhedra in the ***b*** direction by edge-sharing—one of 3.04 Å between two Co_2 ions that share an O_3–$O_{3'}$ edge across a centre of symmetry and the other of 3.15 Å between Co_1 and Co_2 across the shared edge O_1–O_2. The orientations of the cobalt moments are illustrated in figure 4. It can be seen that the Co_2–Co_2 coupling is such that the angle between their moments is approximately 90°, the angle at the O_3 ions being 98.7°. The coupling between the Co_1 and Co_2 ionic moments is principally ferromagnetic by direct exchange, but the angle between the moments of 33(2)° probably reflects the influence of single-ion anisotropy arising through spin–orbit coupling. If we assume that a lowering of the exchange would result in an increase in the inter-moment angle and that the moments would move in the plane they define, we can arrive at their likely orientations due to single-ion anisotropy alone. In the case of Co_1, this is close to the bisector of the octahedral face defined by O_1, O_2 and O_4, whereas for Co_2 it might lie between the ligands O_2 and O_3.

The exchange paths coupling the ***b*** axis chains of edge-sharing oxygen polyhedra are via point-sharing, Co_1–O_4–Co_2, in the ***c*** direction and via the phosphate group Co–O–P–O–Co in the ***a*** direction. It is these latter triple exchange interactions, of the form suggested by Mays (1963), that produce the antiferromagnetic doubling along ***a***, Co_1 ions ***a*** apart (5.06 Å) being linked by two such bridges and Co_2 ions by one. Similar couplings have been found in other antiferromagnetic phosphates such as $LiFePO_4$ (Santoro and Newnham 1967) and $Fe_3(PO_4)_2.4H_2O$ (Forsyth *et al* 1970). The super-

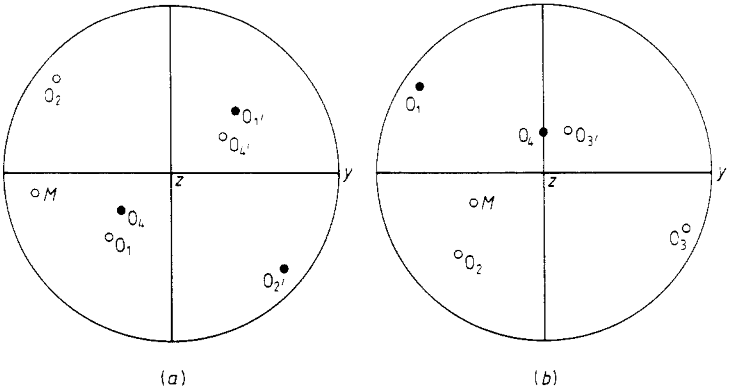

Figure 5. Stereographic projections down [001] of the moment direction, M, in (a) Co_1 and (b) Co_2 relative to the directions of their oxygen ligands, which are six and five in number, respectively.

exchange interaction in the c direction remains ferromagnetic, however, the angle at the O_4 ions being 120.6° and the Co_1–Co_2 distance being 3.64 Å.

References

Anderson J B, Kostiner E, Miller M C and Rea J R 1975 *J. Solid State Chem.* **14** 372
Brown P J and Forsyth J B 1977 *J. Phys. C: Solid State Phys.* **10** 3157
Brown P J, Welford P J and Forsyth J B 1973 *J. Phys. C: Solid State Phys.* **6** 1405
Calvo C J 1963 *J. Phys. Chem. Solids* **24** 141
Clementi E and Roetti C 1974 *At. Data Nucl. Data Tables* **14** 177
Fender B E F, Figgis B N, Forsyth J B, Reynolds P A and Stevens E 1986 *Proc. R. Soc.* A **404** 127
Forsyth J B, Johnson C E and Wilkinson C 1970 *J. Phys. C: Solid State Phys.* **3** 1127
Lisher E J and Forsyth J B 1971 *Acta Crystallogr.* A **27** 545
Nord A G 1974 *Acta Chem. Scand.* A **28** 150
Nord A G and Kierkegaard P 1968 *Acta Chem. Scand.* **22** 1466
Mays J M 1963 *Phys. Rev.* **131** 38
Santoro R P and Newnham R E 1967 *Acta Crystallogr.* **22** 344
Wanklyn B M, Watts B E, Wondre F R and Davidson W 1986 *J. Mater. Sci. Lett.* **5** 499
Wilkinson C 1968 *Phil. Mag.* **17** 609